THE JOURNAL OF BIOLOGICAL CHEMISTRY VOL. 288, NO. 2, pp. 1065–1078, January 11, 2013

Staphylococcus aureus Uses a Novel Multidomain Receptor to Break Apart Human Hemoglobin and Steal Its Heme*

Received for publication, September 14, 2012, and in revised form, October 26, 2012 Published, JBC Papers in Press, November 6, 2012, DOI 10.1074/jbc.M112.419119

Thomas Spirig[‡1,2], G. Reza Malmirchegini[‡1], Jiang Zhang[‡], Scott A. Robson[‡3], Megan Sjodt[‡], Mengyao Liu[§], Kaavya Krishna Kumar[¶], Claire F. Dickson[¶], David A. Gell[¶], Benfang Lei[§], Joseph A. Loo[‡‖], and Robert T. Clubb[‡4]

From the [‡]Department of Chemistry and Biochemistry and the UCLA-Department of Energy Institute for Genomics and Proteomics, UCLA, Los Angeles, California 90095, the [‖]Department of Biological Chemistry, David Geffen School of Medicine at UCLA, Los Angeles, California 90095, the [¶]Menzies Research Institute, University of Tasmania, 17 Liverpool Street, Hobart, TAS 7000, Australia, and the [§]Department of Veterinary Biology, Montana State University, Bozeman, Montana 77005

Background: During infections, *Staphylococcus aureus* acquires heme-iron from human hemoglobin using the receptor proteins IsdH and IsdB.
Results: A conserved multidomain unit in IsdH and IsdB synergistically captures heme and destabilizes the hemoglobin tetramer.
Conclusion: Receptor domain synergy and hemoglobin dissociation allow efficient heme uptake by *S. aureus*.
Significance: IsdH and IsdB may represent novel targets for antibiotics that limit microbial access to iron.

Staphylococcus aureus is a leading cause of life-threatening infections in the United States. It requires iron to grow, which must be actively procured from its host to successfully mount an infection. Heme-iron within hemoglobin (Hb) is the most abundant source of iron in the human body and is captured by *S. aureus* using two closely related receptors, IsdH and IsdB. Here we demonstrate that each receptor captures heme using two conserved near iron transporter (NEAT) domains that function synergistically. NMR studies of the 39-kDa conserved unit from IsdH ($IsdH^{N2N3}$, Ala^{326}–Asp^{660}) reveals that it adopts an elongated dumbbell-shaped structure in which its NEAT domains are properly positioned by a helical linker domain, whose three-dimensional structure is determined here in detail. Electrospray ionization mass spectrometry and heme transfer measurements indicate that $IsdH^{N2N3}$ extracts heme from Hb via an ordered process in which the receptor promotes heme release by inducing steric strain that dissociates the Hb tetramer. Other clinically significant Gram-positive pathogens capture Hb using receptors that contain multiple NEAT domains, suggesting that they use a conserved mechanism.

Staphylococcus aureus is a leading cause of lethal hospital- and community-acquired infections in the United States. These infections result in a range of life-threatening diseases, such as pneumonia, meningitis, osteomyelitis, endocarditis, toxic shock syndrome, bacteremia, and sepsis. Highly virulent methicillin-resistant strains of *S. aureus* are now common, which annually cause more deaths in the United States (over 18,500) than any other single infectious agent (1). Iron is an essential nutrient required for *S. aureus* growth and is actively procured from its host during infections. As an innate defense mechanism, humans and other vertebrates exploit this dependence by sequestering the majority of the body's total iron within cells and by binding extracellular iron to transferrin and lactoferrin glycoproteins (2, 3). Iron-protoporphyrin IX (heme), found in the oxygen transport protein hemoglobin (Hb), contains ~75% of the body's total iron. As a result, *S. aureus* and other microbial pathogens have developed elaborate heme acquisition systems to exploit this rich nutrient source.

S. aureus captures heme-iron from human Hb using nine iron-regulated surface determinant (Isd)[5] proteins (4–7). Four Isd proteins are attached to the cell wall and capture Hb, extract its heme, and pass it across the peptidoglycan to the membrane. These proteins include IsdA, IsdB, and IsdH (also known as HarA), which are attached to the cell wall by the SrtA sortase enzyme (8–11), and IsdC, which is attached to the cell wall by the SrtB sortase (12). Biochemical and cellular localization studies indicate that heme capture is mediated by an ordered set of heme transfer reactions. This process is initiated when the IsdH and IsdB proteins exposed on the cell surface bind Hb and remove its heme (8, 11). Heme is then transferred to IsdA, which, in turn, relays it to the IsdC protein buried within the cell wall (11, 13, 14). Holo-IsdC then passes heme to the IsdE-IsdF complex, a transporter that pumps heme across the membrane

* This work was supported, in whole or in part, by National Institutes of Health Grants AI52217 (to R. T. C.), RR020004 (now reassigned as GM103479) (to J. A. L.), and S10RR028893 from the National Center for Research Resources for purchase of the Fourier transform ion cyclotron resonance mass spectrometer. This work was also supported by Swiss National Science Foundation Fellowship PBEZP3–124281 (to T. S.).
The atomic coordinates and structure factors (code 2LHR) have been deposited in the Protein Data Bank (http://wwpdb.org/).
[1] Both authors contributed equally to this work.
[2] Present address: Institute of Molecular Biology and Biophysics, ETH Zurich, Schafmattstr. 20, 8093 Zurich, Switzerland.
[3] Present address: Dept. of Biological Chemistry and Molecular Pharmacology, Harvard Medical School, Boston, MA 02115.
[4] To whom correspondence should be addressed: Dept. of Chemistry and Biochemistry, University of California, Los Angeles, 602 Boyer Hall, Los Angeles, CA 90095. Tel.: 310-206-2334; Fax: 310-206-4749; E-mail: rclubb@mbi.ucla.edu.

[5] The abbreviations used are: Isd, iron-regulated surface determinant; NEAT, near iron transporter; SUMO, small ubiquitin-like modifier; ESI, electrospray ionization; HSQC, heteronuclear single quantum coherence; TOCSY, total correlation spectroscopy; RDC, residual dipolar coupling.

into the cytoplasm. In the cytoplasm, the heme oxygenase IsdG or its paralog, IsdI, degrades the tetrapyrrole ring to release free iron for use by the bacterium (15). A molecular level understanding of the Isd system could facilitate the development of new anti-infective agents that work by disrupting heme uptake, because several studies have shown that its components are required for *S. aureus* virulence (12, 16–19), and related systems are present in a number of other important pathogens, including *Listeria monocytogenes* (20, 21), *Bacillus anthracis* (22), and *Streptococcus pyogenes* (23–25).

In the Isd system, both Hb and heme are captured by near iron transporter (NEAT) domains that are located within the IsdA, IsdB, IsdC, and IsdH proteins. These conserved binding modules are ~125 residues in length and are named for the location of their genes, which are proximal to putative Fe^{3+} siderophore transporter genes (26). Biochemical studies of isolated NEAT domains indicate that they have distinct binding specificities that enable interactions with one or more distinct ligands, including heme, Hb, haptoglobin, and other host proteins. The atomic structures of several isolated NEAT domains have now been determined, revealing the mechanism of heme and Hb binding (27–29). In addition, recent studies have shown that heme transfer from IsdA to IsdC occurs when their NEAT domains transiently associate via an ultra-low affinity hand clasp complex (30, 31).

The first step in heme acquisition is the capture of Hb and the extraction of its heme molecules by IsdH and IsdB. Both receptors are potential targets for the development of novel antibiotics because *isdH* and *isdB* mutant strains of *S. aureus* are reduced in their ability to infect mice (16, 19, 32, 33), and purified antibodies against IsdH and IsdB confer protection from staphylococcal infections in animal models (33). IsdH and IsdB share a significant degree of primary sequence homology, and, unlike other components of the Isd system, they contain multiple NEAT domains. IsdB has been shown to bind Hb and capture its heme at least 150 times faster than the rate at which Hb spontaneously releases heme into the solvent, suggesting that the receptors capture heme via an activated receptor-Hb complex (14, 34). Here we demonstrate that heme capture by IsdB and IsdH is mediated by a conserved structured unit that contains two NEAT domains that are connected by an α-helical linker domain. We show, based on absorbance spectroscopy and electrospray ionization mass spectrometry (ESI-MS) measurements, that the linker domain in IsdH forms a three-helix bundle structure that is essential for efficient heme capture. NMR studies of a 39-kDa polypeptide containing the conserved unit from IsdH indicate that it adopts an extended but ordered structure. A model of the heme extraction process is presented in which IsdH dissociates the Hb tetramer to promote heme release.

EXPERIMENTAL PROCEDURES

Cloning, Protein Expression, and Purification—Plasmids were generated encoding IsdH and IsdB receptor constructs as small hexahistidine-ubiquitin-like modifier (SUMO)-tagged proteins under control of an inducible promoter: pRM208 coding for amino acids 326–660 in IsdH ($IsdH^{N2N3}$), pRM213 coding for amino acids 326–466 in IsdH ($IsdH^{N2}$), pRM214 coding for amino acids 466–660 in IsdH ($IsdH^{linker\text{-}N3}$), pRM234 coding for amino acids 326–543 in IsdH ($IsdH^{N2\text{-}linker}$), pRM219 coding for amino acids 467–543 in IsdH ($IsdH^{linker}$), and pRM221 coding for amino acids 544–600 in IsdH ($IsdH^{N3}$). Briefly, the DNA was amplified from the *S. aureus* RN4220 genome by polymerase chain reaction (PCR) and cloned into the vector pHis-SUMO using BamHI and XhoI restriction enzymes (35). pRM233 coding for amino acids 326–660 ($IsdH^{N2\text{-}GS\text{-}N3}$) was generated from pRM208 using two-step PCR, such that the linker was replaced with a nine-amino acid artificial linker (GSGSGSGSG). The sequence of all plasmids was verified by DNA sequencing. Generation of the plasmid pRM216 coding for amino acids 326–660 in IsdH with an alanine substitution of Tyr^{642} ($Isd^{N2N3(Y642A)}$) has been described earlier (36). Protein expression in *Escherichia coli* BL21(DE3) cells (New England BioLabs) transformed with the overexpression plasmids in LB/kanamycin (50 μg/ml) was induced with 1 mM isopropyl-β-D-thiogalactoside for 4 h at 37 °C. For production of isotopically labeled [^{13}C,^{15}N]protein, the cells were grown in M9 minimal medium containing $^{15}NH_4Cl$ and [^{13}C]glucose (Cambridge Isotope Laboratories). The bacterial cells were harvested by centrifugation, resuspended in 50 mM NaH_2PO_4, 300 mM NaCl, pH 7.0, and ruptured by sonication. The cell debris was removed by centrifugation, and the supernatant containing the SUMO-tagged proteins was purified using a Co^{2+}-chelating column (Thermo Scientific). After cleavage of the fusion proteins with ULP1 protease for 2 h at 4 °C, they were reapplied to the Co^{2+} chelating column to remove the protease and cleaved SUMO-affinity tag. The receptor proteins were further purified by gel filtration on a Superdex 75 column (GE Healthcare) equilibrated with 20 mM NaH_2PO_4, 50 mM NaCl, pH 6.0. Heme contents of holo- and apoproteins were determined with the pyridine hemochrome assay, and homogeneous apo forms of the heme-binding proteins were generated by extraction with methyl ethyl ketone (37). Expression and purification of [U-^{2}H,^{13}C,^{15}N]$Isd^{N2N3(Y642A)}$ was performed according to a previously published protocol (36).

Preparation of Human Hemoglobin—Human blood (30–40 ml) was collected with heparin anticoagulant by a health practitioner following appropriate institutional protocols. Red blood cells were collected by centrifugation at 700 × *g* for 10 min at 4 °C. The cells were washed three times with 0.9% NaCl and bubbled with carbon monoxide (CO) for 5 min. The cells were then collected by centrifugation and lysed by resuspension in five volumes of water, followed by incubation on ice for 30 min. NaCl was added to a final concentration of 0.9%, resulting in aggregation of the membrane fractions into a gelatinous phase, which was removed by centrifugation for 15 min at 9500 × *g*. The supernatant containing Hb was supplemented with 1 mM EDTA and bubbled with CO for 5 min. After adjusting the pH to 6.9, the hemolysate was applied to an SP Sepharose Fast Flow column (GE Healthcare) equilibrated with 10 mM NaH_2PO_4, 1 mM DTT, pH 6.9, and Hb was eluted with 10 mM Tris-HCl, pH 8.5. The fractions containing Hb were pooled, supplemented with 1 mM EDTA, and bubbled with CO for 5 min. Subsequently, the sample was applied to a Q Sepharose Fast Flow column (GE Healthcare) equilibrated with 10 mM Tris-HCl, pH 8.5. Pure Hb was eluted with 30 mM NaH_2PO_4,

pH 6.9, with a yield of 100 mg of protein/ml of blood. Hb concentrations were determined using Drabkin's reagent (Sigma).

Electrospray Ionization Mass Spectrometry and Circular Dichroism Spectroscopy—Purified human Hb and IsdH proteins were prepared in 10 mM ammonium acetate buffer at pH 6.9, subsequently mixed to concentrations of 10 and 20 μM, respectively, and incubated at 25 °C for 1 h. MS measurements of protein samples were performed on a Waters Synapt G1 QTOF mass spectrometer (Waters Corp., Milford, MA) (35). The protein solutions were electrosprayed using Proxeon glass capillary nanoelectrospray emitters at flow rates between 30 and 50 nl/min. Quantification of Hb and Hb-receptor complexes was performed based on the Waters Synapt data by comparing summed peak heights. Higher resolution mass spectrometry experiments were performed using a 15-tesla Fourier transform ion cyclotron resonance instrument (SolariX hybrid Qq-FTMS, Bruker Daltonics, Billerica, MA). Circular dichroism spectra of 0.2 mg/ml $IsdB^{linker}$ and $IsdH^{linker}$ in 10 mM NaH_2PO_4, 50 mM NaF, pH 6.8, were recorded on a JASCO J-715 spectropolarimeter (JASCO Corp.) at 25 °C with a scan rate of 20 nm/min.

Heme Transfer Kinetics and Affinity Measurements—Heme transfer reactions from Hb to $IsdB^{N1N2}$ and various IsdH protein constructs were monitored by following absorbance changes using a conventional spectrophotometer (Shimadzu UV-1700 PharmaSpec), as described previously (14). Human hemoglobin was purchased from Sigma and dissolved in 20 mM $NaPO_4$, pH 7.5, 150 mM NaCl. Briefly, 1 μM holo-Hb (expressed in tetrameric units) was mixed with 10 μM apo-receptor protein in 20 mM $NaPO_4$, pH 7.5, 150 mM NaCl. Entire absorbance spectra were recorded for hemin transfer from holo-Hb to apo-$IsdH^{N2N3}$ over time. To compare the heme transfer rates from Hb to the various acceptor proteins, changes in absorbance at 371 and 406 nm were recorded over time at 25 °C for up to 2 h. Apparent rate constants for the heme transfer reactions were obtained by fitting the time courses of the absorbance changes $\Delta A_{406-371}$ to single or double exponential curves with SigmaPlot (Systat Software Inc.). Affinities of $IsdH^{N3}$ and $IsdH^{N2N3}$ for heme were determined by fluorescence spectroscopy as described (38).

NMR Spectroscopy and Solution Structure Determination—NMR spectra of $IsdH^{linker}$ were acquired at 25 °C on cryoprobe-equipped Bruker Avance 500-, 600-, and 800-MHz spectrometers. Backbone and side-chain chemical shift assignments were obtained by analyzing the following experiments: $^{1}H,^{15}N$ HSQC, HNCO, HN(CA)CO, HNCACB, HNCA, CBCA(CO)NH, ^{15}N-edited TOCSY, HNCA, HNHA, HNHB, HBHA(CO)NH, CC(CO)NH, HCCH-TOCSY, HCCH-COSY, ^{15}N-edited NOESY, and ^{13}C-edited NOESY (reviewed in Ref. 39). TALOS+ was used to obtain a majority of the φ and ψ dihedral angle restraints (40). Additional φ dihedral angle restraints were obtained by analyzing HNHA spectra (41). Stereo-specific assignments of methylene protons were obtained by analyzing HNHB and ^{15}N-edited TOCSY spectra. Distance constraints were identified in three-dimensional ^{15}N- and ^{13}C-edited NOESY spectra with mixing times of 125 and 130 ms, respectively. NMR spectra were processed using NMRPipe and analyzed using the CARA and PIPP software packages (42, 43). The program UNIO was used for automated NOE assignments and structure determination of $IsdH^{linker}$ (44). The NOESY data were manually inspected to verify all NOE assignments and identify additional NOE restraints. The structures were improved by iterative rounds of structure calculations in which hydrogen bond restraints, backbone torsion angle restraints obtained from the program TALOS+, and side-chain torsion angle restraints were added (45). A final set of 100 conformers was generated with a standard simulated annealing protocol, as implemented in the program NIH-XPLOR, of which 51 had no NOE, dihedral angle, or scalar coupling violations greater than 0.5 Å, 5°, or 2 Hz, respectively (46). Of these, the 20 conformers with lowest overall energy were chosen to represent the structure of $IsdH^{linker}$. The quality of the structural ensemble was evaluated with PROCHECK and visualized with PyMOL (47, 48). Statistics for the linker structure are presented in Table 1. Details on the NMR experiments used to obtain the backbone chemical shifts of $IsdH^{N2N3(Y642A)}$ have been described (36). $^{1}D_{NH}$ residual dipolar couplings were measured using protein samples partially aligned in PEG C12E5/hexanol using two-dimensional ^{15}N-coupled IPAP ^{1}H-^{15}N HSQC experiments. Steady-state ^{15}N heteronuclear NOE values for the $IsdH^{linker}$ and $IsdH^{N2N3(Y642A)}$ were acquired on cryoprobe-equipped Bruker Avance 600- and 800-MHz spectrometers, respectively. The heteronuclear NOE experiments were carried out in an interleaved manner, with and without proton saturation, and analyzed using the program SPARKY (49).

RESULTS

A Conserved Unit in IsdB and IsdH Containing Two NEAT Domains Rapidly Captures Heme from Hb—The *S. aureus* Hb receptors IsdB and IsdH contain two and three NEAT domains, respectively (Fig. 1*A*). Isolated domains from these receptors have been characterized *in vitro* and bind to either Hb or heme; the $IsdH^{N1}$, $IsdH^{N2}$, and $IsdB^{N1}$ NEAT domains bind to Hb, whereas the C-terminal NEAT domains in both proteins interact with heme ($IsdH^{N3}$ and $IsdB^{N2}$) (32, 38, 50–54). Interestingly, a sequence alignment reveals that IsdB and IsdH share 64% primary sequence identity with one another over a region that encodes two NEAT domains (Figs. 1*A* and 2). This conserved unit contains two NEAT domains that are joined by a ~70-amino acid segment, hereafter referred to as the "linker." In IsdH, the unit corresponds to the N2 and N3 domains, which are homologous to the N1 and N2 domains in IsdB, respectively (Fig. 1*A*, *enclosed* in a *dashed box*). *In vitro*, full-length IsdB rapidly captures heme from Hb (14). To determine if the conserved unit within IsdB and IsdH is responsible for efficient heme capture, UV-visible absorption spectroscopy was used to measure the rate of heme transfer from heme-loaded methemoglobin (MetHb) to either $IsdB^{N1N2}$ (residues Thr^{121}–Asn^{458}, containing the N1 and N2 domains in IsdB) or $IsdH^{N2N3}$ (Ala^{326}–Asp^{660}, containing the N2 and N3 domains in IsdH). All studies were performed under oxidizing conditions, in which heme is in its ferric form. Upon mixing of MetHb with apo-$IsdH^{N2N3}$, a rapid shift of the UV absorbance spectrum of Hb to the heme bound spectrum of $IsdH^{N2N3}$ is observed (Fig. 1*B*). This spectral change is indicative of heme transfer to IsdH and is most pronounced at 371 and 406 nm where the absorb-

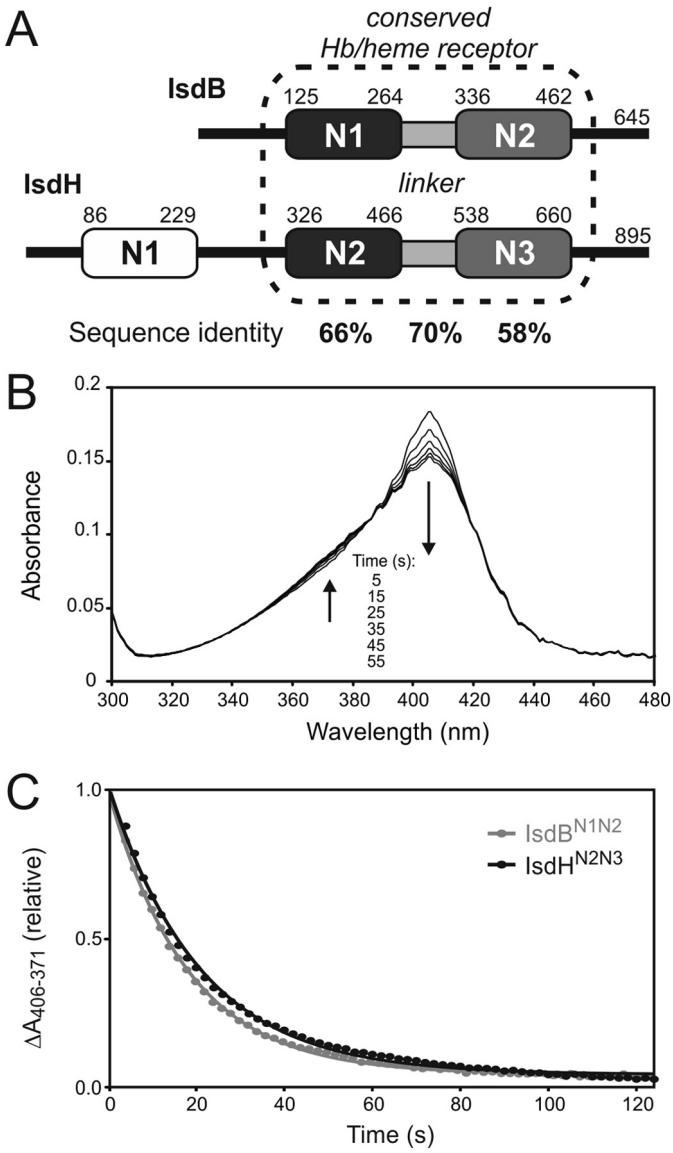

FIGURE 1. **A homolog bidomain unit for heme capture in IsdH and IsdB.** *A*, schematic of the NEAT domains present in *S. aureus* IsdH and IsdB. NEAT domains binding to Hb or heme are *colored* in *black/white* or *gray*, respectively. Sequence identities of functionally homologous NEAT domains as well as the linker connecting them are indicated. *B*, spectral shifts as a function of time after mixing for the reaction of 1 μM holo-Hb with 10 μM apo-IsdH^{N2N3}. *Arrows* indicate the increase and decrease in absorbance over time at 371 and 406 nm, respectively. *C*, time courses of $\Delta A_{406-371}$ for the heme transfer reaction from Hb to IsdH^{N2N3} or IsdB^{N1N2}. The *symbols* and *curves* represent the observed data and the single-exponential fitting curves, respectively, yielding heme transfer rates of 0.048 $\pm$ 0.001 s^{-1} and 0.055 $\pm$ 0.001 s^{-1} for IsdH^{N2N3} and IsdB^{N1N2}, respectively.

ance increases and decreases, respectively. A kinetic analysis of the heme transfer data indicates that IsdB^{N1N2} and IsdH^{N2N3} capture heme from Hb at similar rates, 0.055 $\pm$ 0.001 and 0.048 $\pm$ 0.001 s^{-1}, respectively (Fig. 1*C*). These rates are similar to those measured for intact IsdB and are up to 580 times faster than the rate at which tetrameric Hb spontaneously releases heme into the solvent, suggesting that heme transfer to IsdB and IsdH occurs via a MetHb-receptor complex (14, 34).

To determine if the NEAT domains within IsdH need to be part of the same polypeptide to rapidly extract heme, we measured the rate of heme transfer from MetHb to the isolated N3 domain in the presence and absence of the Hb binding N2 domain (Fig. 3, *A* and *B*). Compared with IsdH^{N2N3}, the isolated heme binding domain IsdH^{N3} (Leu^{544}–Asp^{660}) acquires heme from MetHb very slowly, which is consistent with an indirect transfer mechanism in which heme is first released from MetHb into the solvent before it is acquired by IsdH^{N3} (Fig. 3*B*). The addition of the MetHb binding IsdH^{N2} protein (Ala^{326}–Pro^{466}) in *trans* to this transfer reaction fails to increase the rate of heme transfer from MetHb to IsdH^{N3} (Fig. 3*B*, *N2 + N3*). This indicates that IsdH^{N2} binding to MetHb itself does not perturb its structure so as to promote heme release and subsequent capture by the isolated N3 domain. The presence of the N2 domain also does not significantly alter the heme binding affinity of the N3 domain within IsdH^{N2N3}, because IsdH^{N2N3} and IsdH^{N3} bind heme with similar affinities, K_D values of 3.2 $\pm$ 0.7 and 3.4 $\pm$ 0.6 μM, respectively (Fig. 4). Combined, these data strongly suggest that the N2 and N3 domains of IsdH need to reside within the same polypeptide to efficiently capture heme from Hb. Because IsdB contains this conserved unit, its NEAT domains also presumably synergistically extract heme (Fig. 2).

The NEAT Domains within IsdH and IsdB Are Connected by a Functionally Important Helical Linker—The ~70-amino acid linker segments that connect the NEAT domains in IsdB and IsdH share 70% sequence identity (Fig. 2). To investigate their structure, we purified polypeptides containing this segment from IsdB (IsdB^{linker}, Ser^{263}–Ser^{361}) and IsdH (IsdH^{linker}, Pro^{466}–Val^{564}). Their circular dichroism (CD) spectra indicate that IsdB^{linker} and IsdH^{linker} adopt a helical conformation, which is evident by negative bands in their CD spectra at 222 and 208 nm and a positive band at 193 nm (Fig. 5*A*). This is consistent with secondary structure predictions, which propose that amino acids in this region form several α-helices. To explore the functional role of the linker domain in IsdH, UV-visible absorbance spectroscopy was used to follow heme capture from MetHb. IsdH^{linker} was unable to acquire heme from MetHb (Fig. 3*B*). Moreover, the presence of IsdH^{linker} and IsdH^{N2} did not accelerate the rate at which IsdH^{N3} captures heme from MetHb (Fig. 3*C*, *N2 + linker + N3*). This indicates that the isolated components of the conserved unit in IsdH are unable to associate with one another via non-covalent interactions to form a fully functioning receptor. To further investigate the function of the linker, polypeptides in which the linker was fused to either the N2 (IsdH$^{N2\text{-}linker}$, Ala^{326}–Gln^{543}) or N3 (IsdH$^{linker\text{-}N3}$, Leu^{544}–Asp^{660}) domains were studied. Slow transfer from MetHb to the isolated N3 domain was observed when IsdH$^{N2\text{-}linker}$ was added in *trans*, indicating that MetHb binding by IsdH$^{N2\text{-}linker}$ did not significantly promote heme release and subsequent capture by IsdH^{N3}. Similarly, IsdH$^{linker\text{-}N3}$ captures heme slowly from MetHb in either the presence or absence of IsdH^{N2}, indicating that the presence of the helical linker does not influence the N3 domain's ability to scavenge heme (Fig. 3*C*). To determine if the structure of the linker is important for function, we studied IsdH$^{N2\text{-}GS\text{-}N3}$, which replaces the linker with a nine-residue glycine- and serine-rich polypeptide (GSGSGSGSG). Spectroscopic measurements reveal that IsdH$^{N2\text{-}GS\text{-}N3}$ captures heme slowly from MetHb at a rate that is similar to that of the isolated N3 domain

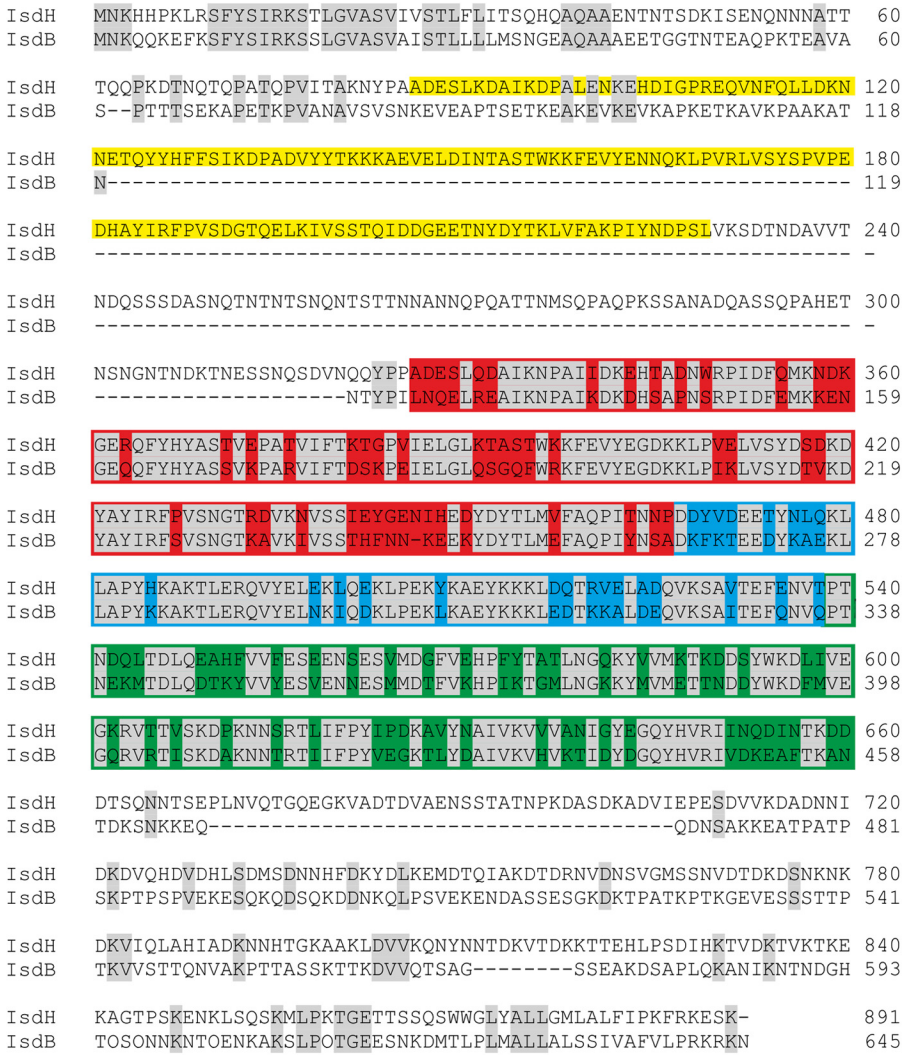

FIGURE 2. **Alignment of IsdH and IsdB.** A primary sequence alignment of IsdH (Q99TD3) and IsdB (Q7A656) was generated using ClustalW (69). Conserved residues are indicated by *gray boxes*. The predicted NEAT domains IsdH^{N1}, IsdH^{N2}/IsdB^{N1}, and IsdH^{N3}/IsdB^{N2} are *highlighted* by *yellow*, *red*, and *green boxes*, respectively. The IsdH and IsdB linker domains are indicated by *blue boxes*.

(Fig. 3, compare *B* and *C*). Combined, these data indicate that the NEAT domains in IsdB and IsdH are connected by a helical linker, whose primary function is to properly position the domains so as to specifically facilitate heme transfer from MetHb to the N3 domain.

IsdH Destabilizes Hb to Promote Heme Release—We used ESI-mass spectrometry to investigate the mechanism through which IsdH accelerates heme release from Hb. ESI-MS allows the quantification of different Hb oligomers in the presence and absence of IsdH (55). Hb consists of α- and β-globin chains each bound to a heme. The globins assemble into a noncovalently bound $(\alpha\beta)_2$ tetramer that dissociates into $(\alpha\beta)$ dimers with a dissociation constant (K_D) of 2 μM (56). This is evident from the ESI-MS spectrum of a 10 μM solution of Hb; from the ratio of the signal from the dimer and tetramer ions, the dimer/tetramer ratio is 1:1.4. This is consistent with previously reported studies (57, 58) and validates the use of ESI-MS to estimate the relative abundances of Hb species. ESI-MS spectra of Hb were acquired in the presence or absence of either wild-type IsdH^{N2N3}, IsdH$^{N2\text{-}GS\text{-}N3}$, or IsdH$^{N2N3(Y642A)}$, which contains a Y642A mutation in the N3 domain that disrupts heme binding (Fig. 6, *A*–*D*). In all of the experiments, the receptors were present at a 2-fold molar excess relative to Hb (expressed in tetrameric units). The ESI-MS data are summarized in Fig. 6*E*, which shows a histogram plot of the relative abundances of the various forms of Hb (the sum of the monomeric α- or β-globins (*M*); $(\alpha\beta)$ dimer (*D*); and $(\alpha\beta)_2$ tetramer (*T*)), as well as receptor-bound forms of the $(\alpha\beta)_2$ tetramer (*T*:*R*), and $(\alpha\beta)$ dimer (*D*:*R*). Incubation of IsdH^{N2N3} with Hb substantially reduces the amount of dimeric and tetrameric Hb, which is converted into monomeric globins. This is consistent with previous studies that have shown that Hb dissociates into its component globins upon heme removal (58, 59). Because substoichiometric amounts of the receptor were used, Hb dissociation is not complete, leaving mostly a mixture of dimeric Hb and the $(\alpha\beta)$ dimer-receptor complex. Importantly, after the IsdH^{N2N3} addition, most of the Hb tetramer disappears, and very little $(\alpha\beta)_2$ tetramer-receptor complex is formed. This indicates that receptor binding and/or heme removal significantly destabilizes the tetramer.

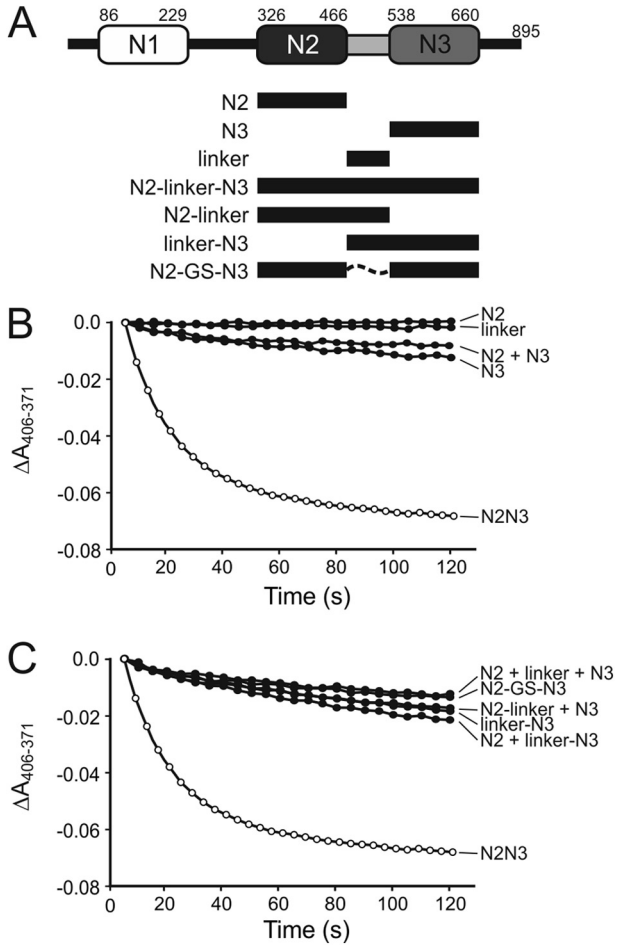

FIGURE 3. **Heme transfer by various fragments of IsdH.** *A*, a schematic of the different fragments of IsdH used for heme transfer experiments. *B* and *C*, time courses for the heme transfer reaction from 1 μM holo-Hb to 10 μM apo-IsdH^{N2N3}. Various IsdH receptor fragments as well as combinations thereof and the linker deletion construct IsdH$^{N2\text{-}GS\text{-}N3}$ are displayed. Heme transfer is followed by monitoring $\Delta A_{406-371}$ over 2 min.

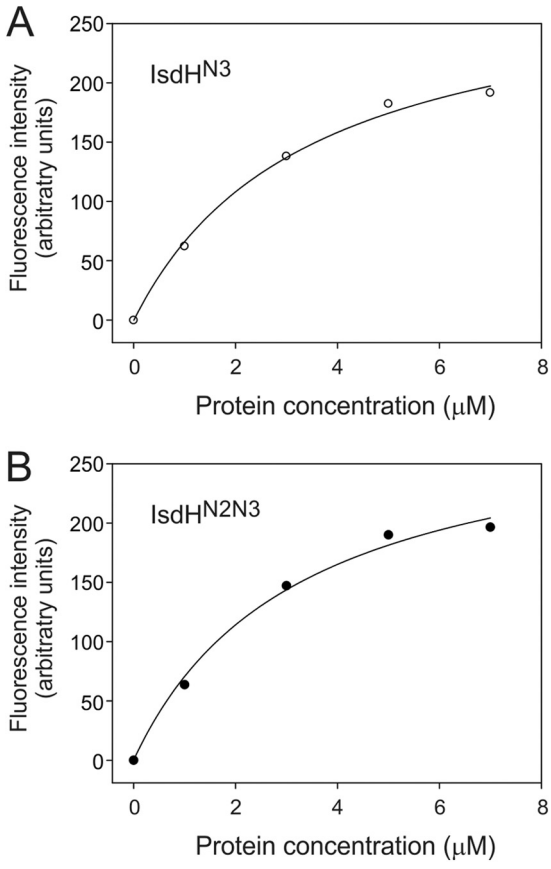

FIGURE 4. **Heme binding properties of IsdH^{N3} and IsdH^{N2N3}.** Protoporphyrin binding of IsdH^{N3} (*A*) or IsdH^{N2N3} (*B*) was measured following zinc-protoporphyrin IX fluorescence as a function of protein concentration (38). The *solid lines* represent best fits of the data yielding dissociation constants (K_D) of 3.4 $\pm$ 0.6 μM and 3.2 $\pm$ 0.7 μM for IsdH^{N3} and IsdH^{N2N3}, respectively.

To gain insight into the role of the linker and heme binding in the acquisition process, ESI-MS spectra of Hb in the presence of IsdH$^{N2\text{-}GS\text{-}N3}$ or IsdH$^{N2N3(Y642A)}$ were acquired. Unlike the wild-type receptor, when the IsdH$^{N2\text{-}GS\text{-}N3}$ linker mutant is incubated with Hb, the majority of the receptor binds to the $(\alpha\beta)_2$ tetramer to form a $(\alpha\beta)_2$-IsdH$^{N2\text{-}GS\text{-}N3}$ complex, and a significant fraction of the tetramer remains intact (Fig. 6*E*). Moreover, smaller amounts of Hb are converted to its monomeric globins, whereas roughly similar amounts of $(\alpha\beta)$ dimer and $(\alpha\beta)$ dimer-receptor complex are present. The absence of monomeric globins is compatible with the kinetic data that showed that IsdH$^{N2\text{-}GS\text{-}N3}$ extracted heme from Hb inefficiently. The fact that the linker mutant does not disrupt the tetramer suggests that it adopts a unique structure as compared with the wild-type protein, such that the mutant receptor can no longer impart sufficient structural strain to rupture the tetramer. To determine if the receptor needs to bind heme in order to dissociate the Hb tetramer, we studied IsdH$^{N2N3(Y642A)}$, which contains a Y642A mutation in the N3 domain that disrupts heme binding. When Hb is incubated with IsdH$^{N2N3(Y642A)}$, the amount of tetrameric Hb is significantly reduced as a result of its conversion into the $(\alpha\beta)$-IsdH$^{N2N3(Y642A)}$ complex. However, only small amounts of monomeric globin are produced. This suggests that heme removal from the tetramer by the receptor is not required to dissociate it into its dimeric state. However, heme removal appears to be required to convert Hb into its monomeric units. A working model of the extraction process is presented under "Discussion."

Structure of the Linker Domain—To gain a better understanding of the molecular basis of heme capture, we determined the NMR solution structure of IsdH^{linker} (Protein Data Bank accession code 2LHR). The NMR spectra of IsdH^{linker} are well resolved, enabling nearly complete ^{1}H, ^{13}C, and ^{15}N resonance assignments (Fig. 5*B*). A total of 1793 experimentally derived restraints were used to determine the structure, including 1469 interproton distance restraints, 118 dihedral angle restraints, 54 $^{3}J_{HN\alpha}$ restraints, and 152 ^{13}C secondary shift restraints. An ensemble of 20 conformers representing the structure of IsdH^{linker} is displayed in Fig. 7*A*. The structure is well defined by the NMR data; the backbone and heavy atom coordinates of the structured residues Val^{470}–Val^{531} can be superimposed with a root mean square deviation of 0.42 $\pm$ 0.10 and 0.87 $\pm$ 0.07 Å, respectively (experimental and structural parameters are presented in Table 1).

The linker forms a three-helix bundle that is composed of helices α1 (Asp^{471}–Lys^{486}), α2 (Leu^{490}–Lys^{503}), and α3

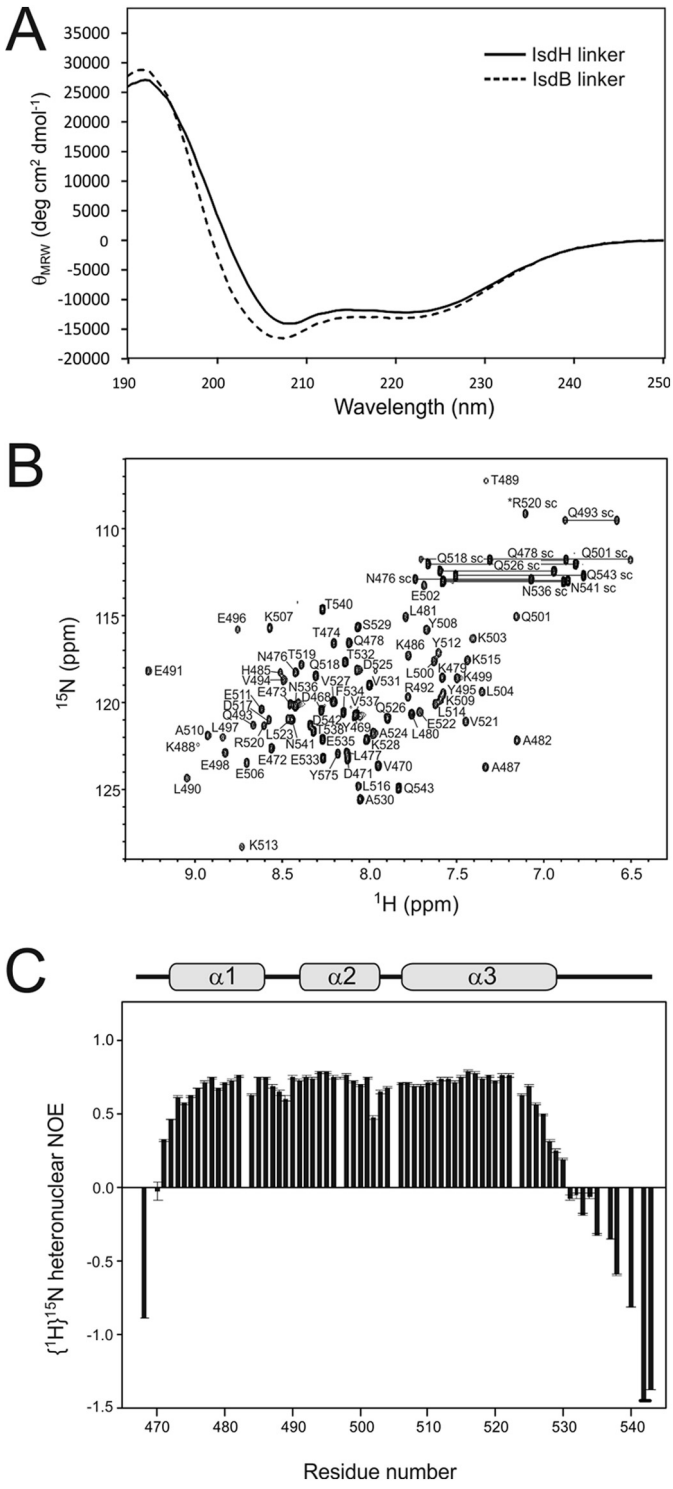

FIGURE 5. **The IsdH and IsdB linkers fold into soluble α-helical domains.** *A*, far-UV CD spectra of the linker domains of IsdH (*solid*) and IsdB (*dashed*). The strongly negative CD signals with minima around 208 and 222 nm are indicative of α-helical proteins. *B*, ^{1}H-^{15}N HSQC spectrum of 1.1 mM ^{15}N-labeled IsdH^{linker} acquired at 800 MHz. The amino acid assignment for each cross-peak is indicated with *one-letter code* and *residue number*. Amide $^{\delta}NH_2$ of Asn and $^{\gamma}NH_2$ of Gln are connected by *lines* and denoted as *sc* for side chain. An *asterisk* indicates the cross-peak from the $^{\epsilon}$NH of Arg^{520}, which was folded in the ^{15}N dimension. *C*, {^{1}H}-^{15}N heteronuclear NOE data of the IsdH^{linker}. The peak intensity ratio between spectra with and without ^{1}H saturation as a function of the residue number is shown. The average heteronuclear NOE values and S.D. values of two experiments are displayed, and the location of the three α-helices is indicated at the *top*.

(Glu^{506}–Ala^{530}) (Fig. 7*B*). In the bundle, the long axes of the helices are co-linear and are connected by short reverse turns. The structure is stabilized by a hydrophobic core that is formed by nine leucine and tyrosine residues (Leu^{477}, Leu^{480}, Leu^{481}, Tyr^{484}, Leu^{497}, Leu^{500}, Leu^{504}, Tyr^{508}, and Tyr^{512}; Fig. 7*C*). Although each helix contributes residues to the hydrophobic core, helix α3 is longer than the other helices, such that its C terminus projects from the bundle. This region and residues immediately following it presumably facilitate interactions with the N3 domain in the intact receptor (see below). {^{1}H}^{15}N heteronuclear NOE measurements are compatible with the structure because residues Val^{470}–Val^{531}, whose coordinates are precisely defined in the ensemble, exhibit large magnitude NOE values, indicating that they are immobile on the picosecond time scale (Fig. 5*C*).

IsdH^{N2N3} Adopts an Extended but Ordered Multidomain Structure—We used NMR to investigate the structure and dynamics of IsdH$^{N2N3(Y642A)}$. It is structurally identical to the wild-type protein based on its HSQC spectrum but is reduced in its ability to bind heme. Previously, we sequence-specifically assigned the chemical shifts of its backbone atoms (36). To learn whether the domains form a rigid unit within IsdH$^{N2N3(Y642A)}$, we measured {^{1}H}^{15}N heteronuclear NOE relaxation parameters. As shown in Fig. 8*A*, residues spanning the N2, linker, and N3 domains exhibit positive and mostly uniform {^{1}H}^{15}N heteronuclear NOEs, which indicates that they are structurally ordered. Notably, residues that connect the domains also exhibit positive NOEs. Because some of these residues are unstructured in the isolated linker polypeptide (Fig. 5*C*), this suggests that in the context of IsdH$^{N2N3(Y642A)}$, they form stabilizing interactions with residues located in the N2 and/or N3 domains and that the domains form a single structured unit.

Although the structure of the full receptor is unknown, the structures of the isolated linker and N3 domains are known, and the structure of the N2 domain can be accurately modeled using the previously determined NMR and crystal structures of IsdH^{N1}, which shares 54% sequence identity with N2 (50, 51, 53). To determine whether the domains undergo major structural changes upon incorporation into IsdH^{N2N3}, we measured ^{15}N-^{1}H residual dipolar couplings ($^1D_{NH}$ RDCs) in a sample of IsdH^{N2N3} partially aligned in pentaethylene glycol monododecyl ether ($C_{12}E_5$ PEG)/hexanol. The $^1D_{NH}$ data provide information about the angle of each backbone N–H bond relative to an alignment tensor. The compatibility of the individual domain structures with the RDC data was evaluated by plotting the back-calculated *versus* experimental $^1D_{NH}$ values (Fig. 9). There is good agreement between the experimental data and the individual structures of the N2, linker, and N3 domains, which have calculated *Q*-factors of 0.28, 0.10, and 0.23, respectively. This indicates that incorporation of the domains into IsdH^{N2N3} does not significantly alter their structure and is consistent with our previously reported C_α and C_β backbone secondary chemical shifts of IsdH^{N2N3}, which suggested that the domains have similar secondary structures in isolation and when incorporated into IsdH^{N2N3} (36).

The chemical shifts of IsdH$^{N2N3(Y642A)}$ and polypeptides containing its isolated domains were compared with the aim of

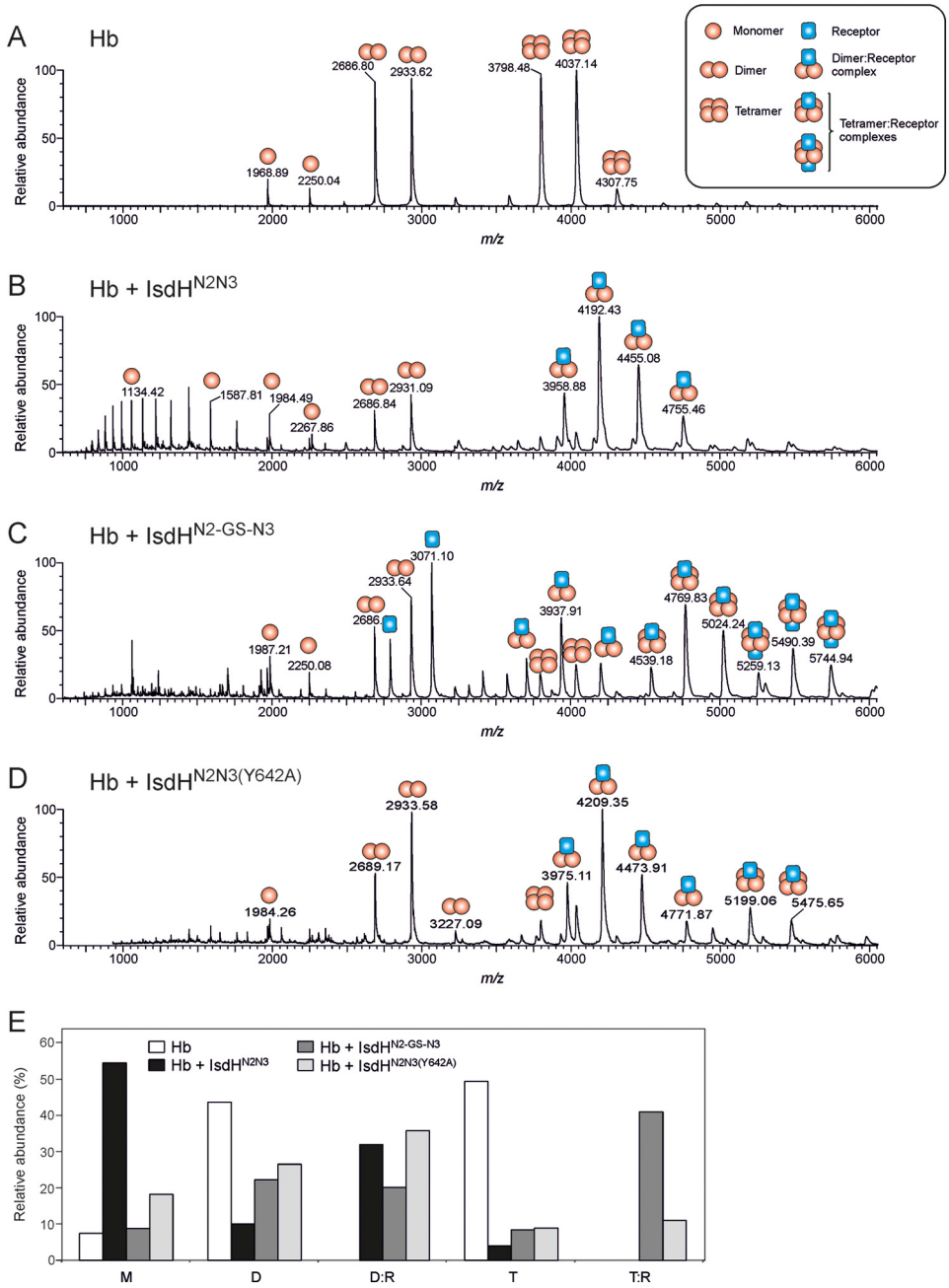

FIGURE 6. **ESI-MS analysis of Hb dissociation by the IsdH receptor.** Positive MS spectra are shown for 10 μM Hb (*A*) and 10 μM Hb in the presence of either 20 μM IsdH^{N2N3} (*B*), IsdH$^{N2\text{-}GS\text{-}N3}$ (*C*), or IsdH$^{N2N3(Y642A)}$ (*D*). The most prominent peaks corresponding to monomeric, dimeric, or tetrameric Hb as well as their complexes with the receptor proteins are *labeled* by the indicated *symbols*. *E*, relative amounts of the different Hb oligomeric states, IsdH receptor proteins, and complexes thereof were quantified from ESI-MS spectra when 10 μM Hb was added to either 20 μM apo-IsdH^{N2N3} (*black*), 20 μM apo-IsdH$^{N2\text{-}GS\text{-}N3}$ (*dark gray*), or 20 μM apo-IsdH$^{N2N3(Y642A)}$ (*light gray*). 10 μM Hb was run as a control (*white*). *M*, monomer; *D*, dimer; *DR*, dimer-receptor complex; *T*, tetramer; *TR*, tetramer-receptor complex.

learning if the domains interact with one another in the context of IsdH$^{N2N3(Y642A)}$. Fig. 8*B* shows an overlay of the secondary chemical shifts of IsdH$^{N2N3(Y642A)}$ and IsdH^{linker}. Similar secondary chemical shifts were observed for the structured part of the linker, suggesting that its conformation is preserved in IsdH$^{N2N3(Y642A)}$. Average chemical shift differences of the backbone amide signals of isolated linker and the corresponding residues in IsdH^{N2N3} are displayed in Fig. 8*C*. In general, small chemical shift differences were observed for residues in the core helices of the linker, indicating that they do not form a molecular surface that interacts with the N2 or the N3 domains. However, significant chemical shift differences in the linker occur for residues located at the beginning of helix α2 (Leu^{490}–Arg^{492}) and at its N terminus (Asp^{468}-Glu^{472}, Thr^{474}–Tyr^{475}) and C terminus (Gln^{526}–Ser^{529}, Val^{531}–Thr^{538}, Thr^{540}–Gln^{543}). Mapping these changes onto the NMR structure of the linker reveals that they reside at distinct ends of the domain (Fig. 8*D*). This is consistent with residues at the beginning of helix α2 and the N terminus of the linker contacting the N2 domain, while residues at the C-terminal end interact with the

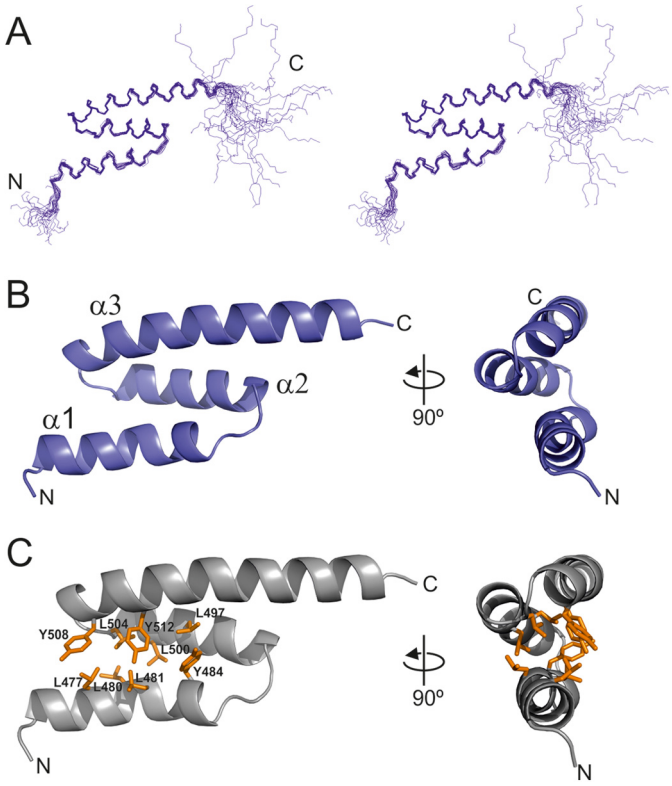

FIGURE 7. **NMR solution structure of IsdH^{linker}.** *A*, *cross-eyed stereo view representation* of the ensemble of 20 lowest energy structures. The coordinates were superimposed by aligning the backbone N, C_{α}, and C′ atoms of residues Val^{470}–Asp^{531}. *B*, *ribbon diagram* of the structured part encompassing residues Val^{470}–Asp^{531} of the lowest energy conformer of IsdH^{linker}. The view on the *left* is in a similar orientation as shown in *B*, whereas the structure on the *right* has been rotated by 90°. The α helices are *labeled* α1–α3. *C*, location of the residues of the hydrophobic core of IsdH^{linker}. A *ribbon diagram* of the structured part encompassing residues Val^{470}–Asp^{531} of the linker structure is shown. The nine residues that form the hydrophobic core are indicated, and heavy atoms of their side chains are shown in *stick representation*.

N3 domain. Interestingly, comparison of the secondary chemical shifts suggests that helix α3 in the linker domain is lengthened at its C terminus when it is incorporated into IsdH^{N2N3} (Fig. 8*B*). Moreover, residues immediately following this segment, based on their secondary chemical shifts, do not participate in regular secondary structure when located in IsdH^{N2N3} but are nevertheless highly ordered, based on the heteronuclear NOE data (Fig. 8*A*). To further ascertain whether the domains in IsdH^{N2N3} might be significantly interacting with one another in IsdH^{N2N3}, we produced ^{15}N samples of IsdH^{N2} and IsdH^{N3}. The ^{1}H-^{15}N HSQC spectrum of IsdH^{N2} is well resolved and, when overlaid with the spectrum of IsdH^{N2N3}, reveals very similar chemical shifts (data not shown). This suggests that, in the context of IsdH^{N2N3}, the N2 domain does not contain a large contact surface that interacts with the remainder of the protein. A similar analysis using ^{15}N-labeled IsdH^{N3} was also attempted but did not prove fruitful because the cross-peaks in its spectrum are partially broadened, presumably because of protein aggregation. Combined, the absence of extensive interaction surfaces in the linker and N2 domains suggests that, while ordered, IsdH^{N2N3} does not adopt a compact structure.

TABLE 1

Structural statistics for the solution structure of IsdH linker domain

The notation of the NMR structures is as follows. ⟨SA⟩ are the final 20 simulated annealing structures; (SA) is the average energy-minimized structure. The number of terms for each restraint is given in parentheses.

	⟨SA⟩[a]	(SA)
Root mean square. deviations		
NOE interproton distance restraints (Å) (1469)	0.046 ± 0.002	0.051
Dihedral angle restraints (degrees)[b] (118)	0.072 ± 0.099	0.306
$^{3}J_{HN}$[a] coupling constants (Hz) (54)	0.532 ± 0.018	0.543
Secondary ^{13}C shifts (ppm)		
13C$_{\alpha}$ (76)	1.212 ± 0.206	1.267
^{13}C$_{\beta}$ (76)	0.816 ± 0.206	0.791
Deviations from idealized covalent geometry		
Bonds (Å)	0.0044 ± 0.0002	0.0174
Angles (degrees)	0.623 ± 0.028	1.538
Impropers (degrees)	0.492 ± 0.031	1.181
PROCHECK results (%)[c]		
Most favorable region	96.7 ± 2.8	96.7
Additionally allowed region	3.3 ± 2.8	3.3
Generously allowed region	0.0 ± 0.0	0.0
Disallowed region	0.0 ± 0.0	0.0
Coordinate precision (Å)[d]		
Protein backbone	0.42 ± 0.10	
Protein heavy atoms	0.87 ± 0.07	

[a] None of the structures exhibits distance violations greater than 0.5 Å, dihedral angle violations greater than 5°, or coupling constant violations greater than 2 Hz.
[b] Experimental dihedral angle restraints comprised 48 φ, 48 ψ, and 16 χ_1 angles.
[c] PROCHECK-NMR data include residues Val^{470}–Val^{531} of the linker domain.
[d] The coordinate precision is defined as the average atomic root mean square deviation of the 20 individual simulated annealing structures and their mean coordinates. The reported values are for residues Val^{470}–Val^{531} of the linker domain.

DISCUSSION

To successfully mount an infection, *S. aureus* and other pathogens acquire the essential nutrient iron from human Hb. Two surface-displayed *S. aureus* receptors capture Hb on the cell surface, IsdB and IsdH. The receptors share a high degree of sequence homology over a region that contains two NEAT domains that are separated by a ~70-amino acid "linker" segment (Figs. 1*A* and 2). The NEAT domains in the conserved units have distinct functions; in each protein, the N-terminal domain binds to Hb, and the C-terminal domain interacts with heme (8, 38). Interestingly, the NEAT domains in IsdB appear to function synergistically, because Lei and colleagues (14) have shown that IsdB captures heme from Hb ~28–250 times faster than proteins that contain only a single NEAT domain. To gain insight into the molecular basis of this synergy, we studied the conserved bi-NEAT domain unit located within IsdH (IsdH^{N2N3}). UV-visible spectroscopy measurements of heme transfer from Hb indicate that IsdH^{N2N3} rapidly acquires the heme of Hb at a rate that is 110–580 times faster than the rate at which Hb spontaneously releases heme into the solvent (IsdH^{N2N3} acquires heme at a rate of 0.048 ± 0.001 s^{-1}, whereas the α and β subunits in tetrameric Hb release heme into the solvent at a rate of ~0.000083 and ~0.00042 s^{-1}, respectively) (34). IsdB and IsdH^{N2N3} capture heme from Hb at a similar rate, compatible with both proteins forming a receptor-Hb complex in which heme is actively removed. These transfer rates may be slower if the heme iron in Hb is in its reduced state, because IsdH^{N3} has been shown to bind ferric heme more tightly than ferrous heme (60). Systematic dissection of IsdH^{N2N3} into its components indicates that its NEAT domains need to be part of the same polypeptide chain in order to rapidly acquire heme from Hb. Moreover, a linker with a *specific* structure and size

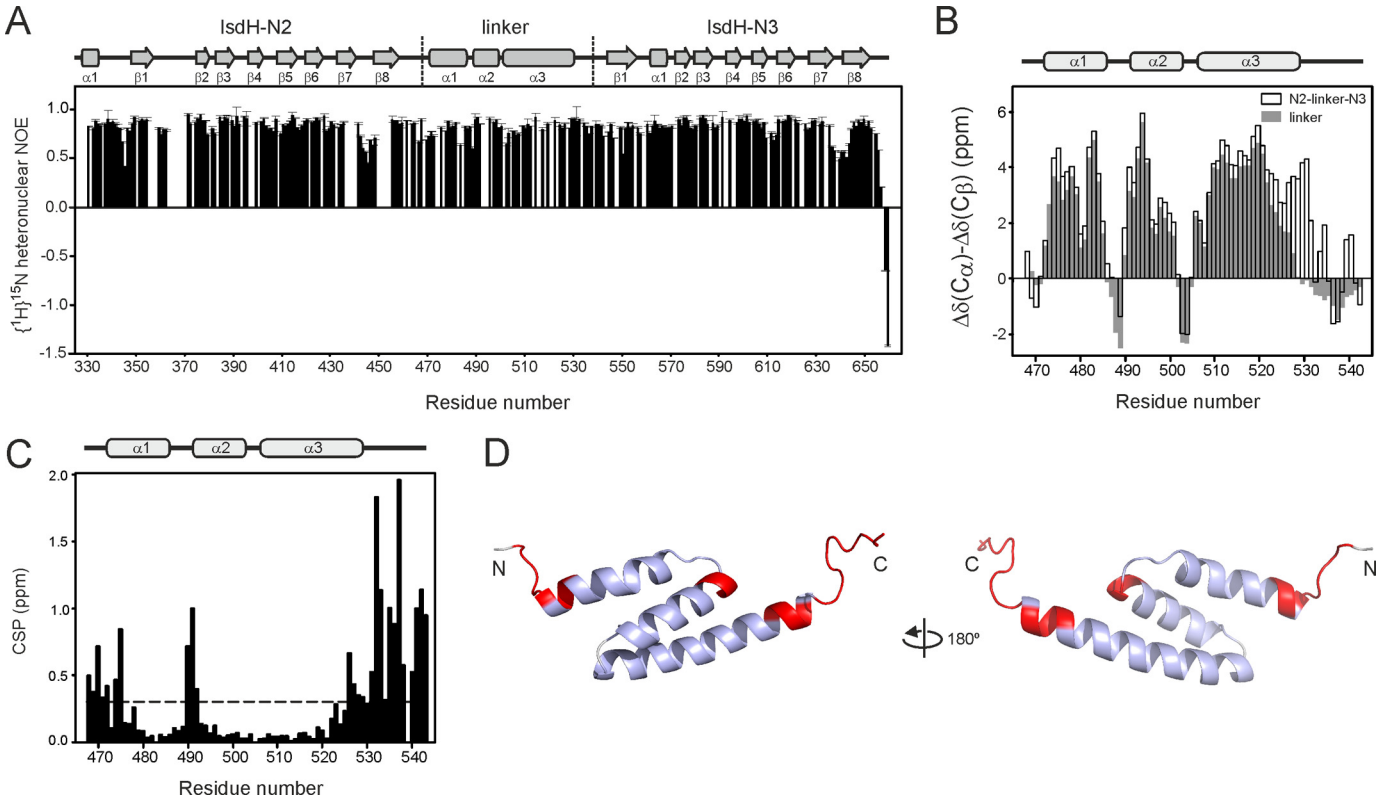

FIGURE 8. **Interactions of IsdH linker with NEAT domains N2 and N3.** *A*, {^{1}H}-^{15}N heteronuclear NOE data of IsdH^{N2N3}. The peak intensity ratio between spectra with and without ^{1}H saturation as a function of the residue number is shown. The average heteronuclear NOE values and S.D. values of two experiments are displayed. The domain boundaries of IsdH^{N2N3} and the location of predicted secondary structure elements are indicated at the *top*. *B*, comparison of the backbone conformations of the isolated IsdH linker region and the corresponding residues in IsdH^{N2N3}. Chemical shift deviations of the linker (*gray bars*) and IsdH^{N2N3} (*open bars*) with respect to the corresponding random coil values are plotted *versus* amino acid residue number, after multiplication with a 1:2:1 weighing function for residues $i - 1/i/i + 1$ (70). Positive values for the chemical shift deviations $\Delta\delta(C_\alpha) - \Delta\delta(C_\beta)$ are indicative of a helical conformation. *C*, average chemical shift differences of the backbone amide signals ($CSP = (\Delta\delta_H^2 + (\Delta\delta_N/6.49)^2)^{1/2}$) of isolated IsdH^{linker} and the linker in the context of the functional receptor IsdH^{N2N3}. *D*, mapping of the perturbed residues on *ribbon diagrams* of the linker. The residues with $CSP > 0.3$ ppm are *highlighted* in *red*.

that connects the domains is required for efficient heme capture; an IsdH$^{N2\text{-}GS\text{-}N3}$ mutant in which the linker is replaced with a glycine-serine nonapeptide acquires heme slowly from Hb.

IsdH^{N2N3} adopts an ordered elongated dumbbell-shaped structure in which its NEAT domains are separated by a helical linker domain. The NMR structure of the linker domain (called IsdH^{linker}) reveals that it adopts a three-helix bundle. First observed in the IgG-binding domain of *S. aureus*, three-helix bundles serve as robust scaffolds for molecular recognition and are ubiquitously found in structural proteins, enzymes, and DNA-binding proteins (61, 62). Because the N and C termini in IsdH^{linker} are positioned at opposite ends of the bundle, in the context of the IsdH^{N2N3} receptor, the linker domain presumably acts as a spacer that holds the N2 and N3 domains apart from another by ~40 Å. This is compatible with the assigned NMR spectra of the intact 39-kDa IsdH^{N2N3} receptor, because a comparison with the NMR spectra of IsdH^{linker} reveals that only residues located at the ends of the helical bundle near the connection points to the N2 and N3 domains exhibit large chemical shift differences. Moreover, the NMR chemical shifts of residues in the isolated IsdH^{N2} domain and IsdH^{N2N3} are similar, suggesting that N2 is not involved in extensive interdomain interactions in the structure of IsdH^{N2N3}. Interestingly, although IsdH^{N2N3} adopts an elongated structure, the domains do not appear to be connected by flexible loops. Inspection of the heteronuclear NOE data of IsdH^{N2N3} reveals nearly uniform values over the length of the polypeptide, including amino acids that connect the domains. Notably, several residues at the N and C termini of the linker domain that are unstructured in the isolated IsdH^{linker} become ordered when they are located in IsdH^{N2N3} (in IsdH^{N2N3}, 2 and 11 residues preceding and following the linker domain, respectively, exhibit elevated NOE values in IsdH^{N2N3} as compared with IsdH^{linker}). Thus, the three domains within IsdH^{N2N3} adopt an extended conformation in which their positioning is fixed with respect to one another. IsdB can be assumed to adopt a similar structure because it shares significant sequence homology with IsdH^{N2N3}, and we have shown that its linker region also adopts a helical conformation.

From the ESI-MS data, IsdH^{N2N3} extracts heme from Hb via the ordered process shown in Fig. 10*A*. On the cell surface, IsdB and IsdH can be expected to encounter Hb in its $(\alpha\beta)_2$ tetrameric and $\alpha\beta$ dimeric forms, whose relative abundance depends on protein concentration. When IsdH^{N2N3} binds to the $(\alpha\beta)_2$ tetramer, it promotes its dissociation into $\alpha\beta$ dimers, which is presumably caused by receptor-induced steric strain that ruptures the weaker $\alpha_1\beta_2$ interface of the tetrameric Hb (63). Dimer formation is expected to facilitate heme transfer to IsdH^{N2N3} because dimeric Hb releases heme more readily than

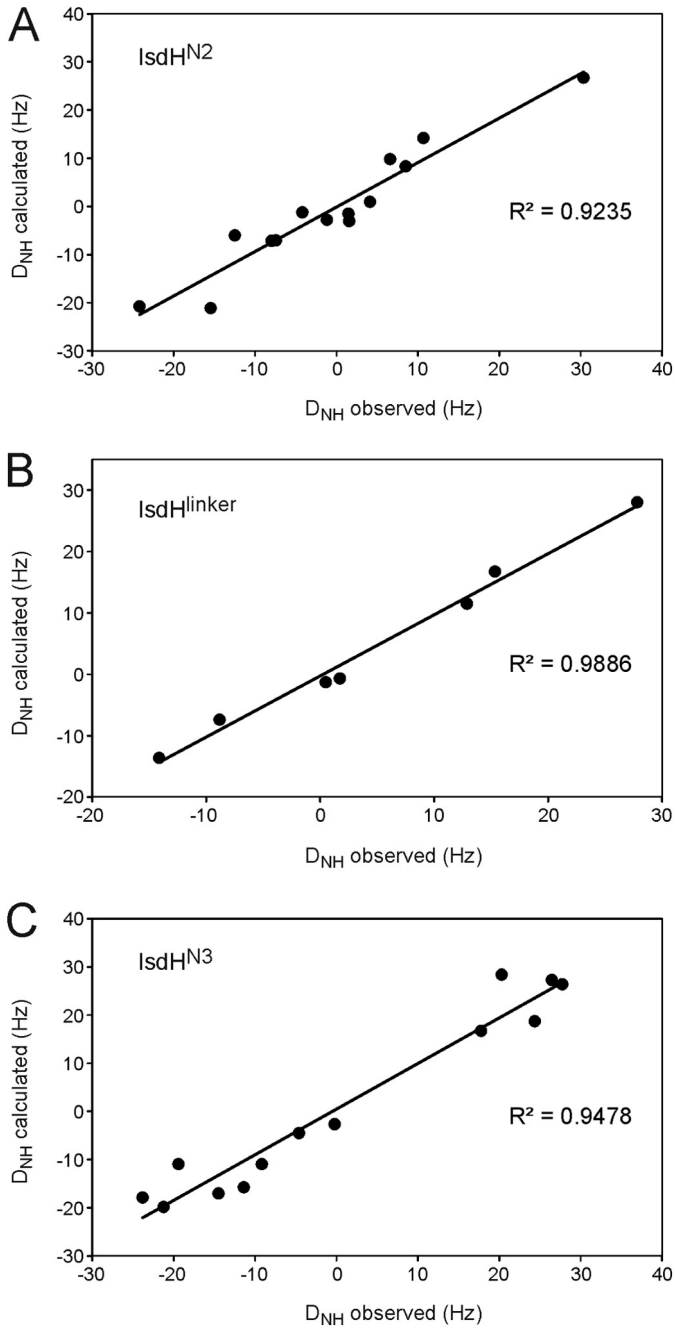

FIGURE 9. **Comparison of experimental and back-calculated RDC values of backbone amide protons in IsdH$^{N2N3(Y642A)}$.** *A*, observed $^1D_{NH}$ RDCs for the N2 domain were plotted *versus* back-calculated RDCs from a homology model of IsdH^{N2}. *B*, experimentally measured $^1D_{NH}$ RDCs for the linker domain were plotted *versus* back-calculated RDCs from the solution structure of the isolated linker. *C*, observed $^1D_{NH}$ RDCs for the N3 domain were plotted *versus* back-calculated RDCs from the crystal structure of IsdH^{N3} (Protein Data Bank entry 2Z6F). The correlation factors *R* are indicated in the plots.

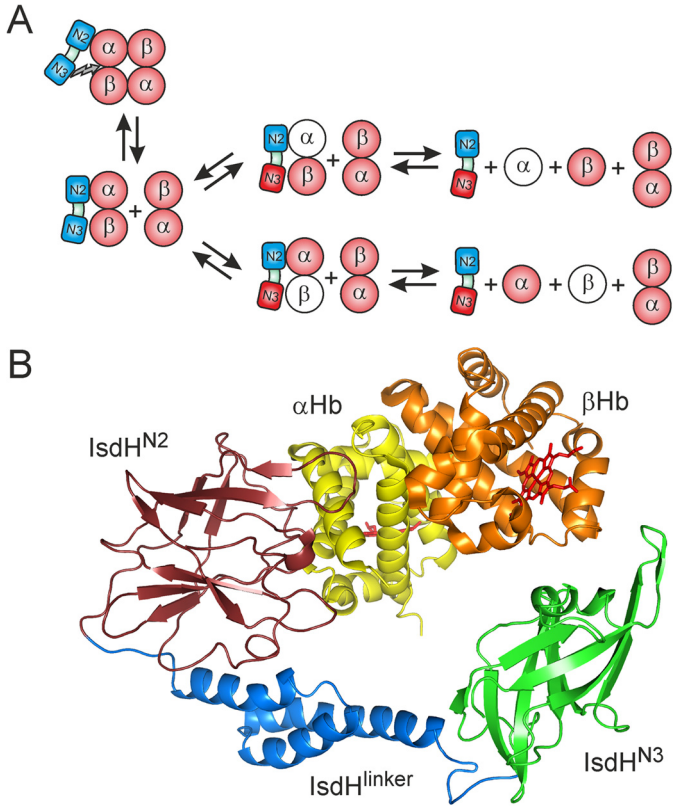

FIGURE 10. **Model of heme extraction by IsdH.** *A*, a model for the mechanism of heme acquisition by the surface receptor IsdH^{N2N3}. A schematic diagram shows the binding equilibria involved in the extraction process. Wild-type IsdH^{N2N3} binds to the α chain of Hb promoting its dissociation into ($\alpha\beta$) dimers. Heme acquisition by the receptor protein results in further dissociation of Hb into its monomeric subunits. See "Discussion" for details. *B*, a model of IsdH^{N2N3} in complex with Hb. IsdH^{N2} (*red*) was modeled based on the solution structure of IsdH^{N1} (Protein Data Bank entry 2H3K). The complex model with Hb was generated by superposition over the crystal structure of the IsdH^{N1}-Hb complex (Protein Data Bank entry 3SZK). A possible orientation of the linker (*blue*) and IsdH^{N3} (*green*; Protein Data Bank entry 2Z6F) allowing productive heme transfer from a Hb ($\alpha\beta$) dimer (*yellow-orange*) to IsdH is indicated. The orientation of the subdomains (N1, linker, and N2) within IsdH^{N2N3} has not been experimentally determined, and only one possible orientation is shown. The protein backbones are shown as schematics. The heme groups in Hb are shown in *stick representation*.

the $(\alpha\beta)_2$ tetramer; compared with the tetramer, the rate of heme loss from the α and β chains in the isolated ($\alpha\beta$) dimer is 2 and 10 times faster, respectively (34). In the second step, heme is transferred from the ($\alpha\beta$) dimer to the N3 domain within the IsdH^{N2N3} receptor. Our data do not reveal which globin chain, if any, serves as the preferred heme donor for IsdH^{N2N3}. It is possible that heme is first removed from the β subunit because it has intrinsically weaker affinity for heme as compared with the α subunit (34). Alternatively, structural distortions induced in the dimer by the receptor may trigger heme transfer from the α chain, creating semi-β Hb from which heme is known to be rapidly released (34). In the final step, after the loss of one of its heme molecules, the ($\alpha\beta$) dimer dissociates completely. Formation of monomeric species is probably driven by the greater tendency of Hb dimers to dissociate (59). As the monomeric α and β chains quickly lose their heme to the environment, both globins could be expected to readily release their ligand to IsdH (34). A similar transfer reaction is expected to occur when IsdH encounters an ($\alpha\beta$) Hb dimer, but it would bypass the need for tetramer dissociation. An alternative heme transfer pathway is also possible. In it, the receptor would remove heme directly from the tetramer or concurrently with tetramer dissociation. Heme removal from the tetramer could be advantageous because it would produce semi-Hb tetramers that are prone to dissociate (64). However, as described immediately below, heme capture from the Hb tetramer is not an obligate step in the transfer reaction.

Several lines of evidence indicate that binding of the $IsdH^{N2N3}$ receptor to tetrameric Hb induces steric strain in Hb that causes it to dissociate into dimers and that this process does not require heme transfer to $IsdH^{N2N3}$ (Fig. 10*A*). The most compelling evidence comes from the ESI-MS data of $IsdH^{N2N3}$ and $IsdH^{N2N3(Y642A)}$, which indicate that both proteins readily disrupt the tetramer. Because $IsdH^{N2N3(Y642A)}$ binds heme with lower affinity, this indicates that structural perturbations in Hb induced by receptor binding are sufficient to cause it to dissociate. This process requires two NEAT domains that are connected by a structured linker because the Hb tetramer does not dissociate when it is bound to an $IsdH^{N2\text{-}GS\text{-}N3}$ mutant in which the linker domain is replaced with a flexible glycine-serine peptide. The idea that an intact bi-NEAT domain receptor is required to dissociate the tetramer is also consistent with a recent crystal structure of the $IsdH^{N1}$-Hb complex, which revealed that binding of the isolated N1 NEAT domain to Hb induced only modest structural changes in Hb (50). As we have shown, $IsdH^{N2N3}$ adopts a rigid structure in its apo state; this suggests that binding of $IsdH^{N2N3}$ to Hb results in atomic overlap between the proteins that causes the tetramer to dissociate. A model of the structure of the $IsdH^{N2N3}$-Hb complex illustrates a possible orientation of the receptor protein on Hb (Fig. 10*B*). The orientation of the subdomains (N1, linker, and N2) within $IsdH^{N2N3}$ has not been experimentally determined, and only one possible orientation is shown. The model was constructed using the NMR structure of $IsdH^{linker}$, the crystal structure of the isolated N3 domain, and a homology model of the N2 domain based on the structure of $IsdH^{N1}$. Based on the recently reported crystal structure of the isolated N1 domain bound to Hb, the N2 domain in $IsdH^{N2N3}$ can be expected to engage the α subunit of Hb via its A-helix (50). Contacts from N2 presumably originate from residues located within surface loops positioned at one end of its β-barrel structure because these residues are conserved in N1 and N2. The relative positioning of the remainder of the $IsdH^{N2N3}$ protein and its contacts to Hb cannot be predicted from our NMR data. However, assuming that $IsdH^{N2N3}$ adopts an extended structure, the N3 domain could, in principle, be positioned adjacent to the heme pockets of either the α or β subunits. Unlike IsdB, the IsdH protein contains an N-terminal NEAT domain (N1) that binds to the α subunit of Hb (Fig. 1*A*) (50). It is possible that the N1 and N2 domains in IsdH simultaneously engage the Hb tetramer via its two α subunits. Alternatively, N1 and N2 may not simultaneously engage the same tetramer. In this scenario, Hb binding by N1 may function to increase the efficiency of heme capture by increasing the local concentration of Hb that is proximal to $IsdH^{N2N3}$. A more detailed understanding of the mechanism of extraction and the origin of molecular strain induced by the receptor on Hb will require studies of the full-length IsdH protein and the structure determination of $IsdH^{N2N3}$ in both its free and Hb-bound states.

We have demonstrated that the NEAT domains within IsdH function synergistically to capture heme from Hb. Interestingly, several other pathogenic species of Gram-positive bacteria display surface proteins implicated in heme capture that contain more than one NEAT domain (26). At present, only a few of these proteins have been characterized biochemically. *S. pyogenes* encodes the membrane-anchored Shr protein, which has two NEAT domains, and, similar to IsdB and IsdH, it has been proposed to acquire heme via a receptor-Hb complex (65, 66). *B. anthracis* produces a Hb hemophore called IsdX2 that contains five NEAT domains (67, 68). All of its domains bind Hb, and some are multifunctional because they can also bind heme. It will be interesting to see if subsets of these domains are also connected by structured linker segments that enable their NEAT domains to function synergistically. Despite the prevalence and importance of multi-NEAT domain proteins in Gram-positive bacteria, this present study is the first to address in detail the possible interactions between NEAT domains, the role of the linker segments, and functional synergy between these regions. Further research will be required to reveal if the mechanism of extraction described here can be generalized to other NEAT-containing Hb receptors. This work could lead to small molecule antibiotics that work by limiting microbial access to heme-iron.

Acknowledgment—We thank Dr. Robert Peterson for assistance with the NMR experiments.

REFERENCES

1. Klevens, R. M., Morrison, M. A., Nadle, J., Petit, S., Gershman, K., Ray, S., Harrison, L. H., Lynfield, R., Dumyati, G., Townes, J. M., Craig, A. S., Zell, E. R., Fosheim, G. E., McDougal, L. K., Carey, R. B., Fridkin, S. K., and Active Bacterial Core surveillance (ABCs) MRSA Investigators (2007) Invasive methicillin-resistant *Staphylococcus aureus* infections in the United States. *JAMA* **298,** 1763–1771
2. Papanikolaou, G., and Pantopoulos, K. (2005) Iron metabolism and toxicity. *Toxicol. Appl. Pharmacol.* **202,** 199–211
3. Ward, P. P., and Conneely, O. M. (2004) Lactoferrin. Role in iron homeostasis and host defense against microbial infection. *Biometals* **17,** 203–208
4. Grigg, J. C., Ukpabi, G., Gaudin, C. F., and Murphy, M. E. (2010) Structural biology of heme binding in the *Staphylococcus aureus* Isd system. *J. Inorg. Biochem.* **104,** 341–348
5. Reniere, M. L., Torres, V. J., and Skaar, E. P. (2007) Intracellular metalloporphyrin metabolism in *Staphylococcus aureus*. *Biometals* **20,** 333–345
6. Skaar, E. P., and Schneewind, O. (2004) Iron-regulated surface determinants (Isd) of *Staphylococcus aureus*. *Stealing iron from heme. Microbes Infect.* **6,** 390–397
7. Ton-That, H., Marraffini, L. A., and Schneewind, O. (2004) Protein sorting to the cell wall envelope of Gram-positive bacteria. *Biochim. Biophys. Acta* **1694,** 269–278
8. Dryla, A., Gelbmann, D., von Gabain, A., and Nagy, E. (2003) Identification of a novel iron regulated staphylococcal surface protein with haptoglobin-haemoglobin binding activity. *Mol. Microbiol.* **49,** 37–53
9. Taylor, J. M., and Heinrichs, D. E. (2002) Transferrin binding in *Staphylococcus aureus*. Involvement of a cell wall-anchored protein. *Mol. Microbiol.* **43,** 1603–1614
10. Clarke, S. R., Wiltshire, M. D., and Foster, S. J. (2004) IsdA of *Staphylococcus aureus* is a broad spectrum, iron-regulated adhesin. *Mol. Microbiol.* **51,** 1509–1519
11. Mazmanian, S. K., Skaar, E. P., Gaspar, A. H., Humayun, M., Gornicki, P., Jelenska, J., Joachmiak, A., Missiakas, D. M., and Schneewind, O. (2003) Passage of heme-iron across the envelope of *Staphylococcus aureus*. *Science* **299,** 906–909
12. Mazmanian, S. K., Ton-That, H., Su, K., and Schneewind, O. (2002) An iron-regulated sortase anchors a class of surface protein during *Staphylococcus aureus* pathogenesis. *Proc. Natl. Acad. Sci. U.S.A.* **99,** 2293–2298
13. Muryoi, N., Tiedemann, M. T., Pluym, M., Cheung, J., Heinrichs, D. E., and

Stillman, M. J. (2008) Demonstration of the iron-regulated surface determinant (Isd) heme transfer pathway in *Staphylococcus aureus*. *J. Biol. Chem.* **283,** 28125–28136
14. Zhu, H., Xie, G., Liu, M., Olson, J. S., Fabian, M., Dooley, D. M., and Lei, B. (2008) Pathway for heme uptake from human methemoglobin by the iron-regulated surface determinants system of *Staphylococcus aureus*. *J. Biol. Chem.* **283,** 18450–18460
15. Skaar, E. P., Gaspar, A. H., and Schneewind, O. (2004) IsdG and IsdI, heme-degrading enzymes in the cytoplasm of *Staphylococcus aureus*. *J. Biol. Chem.* **279,** 436–443
16. Pishchany, G., Dickey, S. E., and Skaar, E. P. (2009) Subcellular localization of the *Staphylococcus aureus* heme iron transport components IsdA and IsdB. *Infect. Immun.* **77,** 2624–2634
17. Pishchany, G., McCoy, A. L., Torres, V. J., Krause, J. C., Crowe, J. E., Jr., Fabry, M. E., and Skaar, E. P. (2010) Specificity for human hemoglobin enhances *Staphylococcus aureus* infection. *Cell Host Microbe* **8,** 544–550
18. Grigg, J. C., Vermeiren, C. L., Heinrichs, D. E., and Murphy, M. E. (2007) Heme coordination by *Staphylococcus aureus* IsdE. *J. Biol. Chem.* **282,** 28815–28822
19. Visai, L., Yanagisawa, N., Josefsson, E., Tarkowski, A., Pezzali, I., Rooijakkers, S. H., Foster, T. J., and Speziale, P. (2009) Immune evasion by *Staphylococcus aureus* conferred by iron-regulated surface determinant protein IsdH. *Microbiology* **155,** 667–679
20. Newton, S. M., Klebba, P. E., Raynaud, C., Shao, Y., Jiang, X., Dubail, I., Archer, C., Frehel, C., and Charbit, A. (2005) The *svpA-srtB* locus of *Listeria monocytogenes*. Fur-mediated iron regulation and effect on virulence. *Mol. Microbiol.* **55,** 927–940
21. Xiao, Q., Jiang, X., Moore, K. J., Shao, Y., Pi, H., Dubail, I., Charbit, A., Newton, S. M., and Klebba, P. E. (2011) Sortase independent and dependent systems for acquisition of haem and haemoglobin in *Listeria monocytogenes*. *Mol. Microbiol.* **80,** 1581–1597
22. Honsa, E. S., and Maresso, A. W. (2011) Mechanisms of iron import in anthrax. *Biometals* **24,** 533–545
23. Liu, M., and Lei, B. (2005) Heme transfer from streptococcal cell surface protein Shp to HtsA of transporter HtsABC. *Infect. Immun.* **73,** 5086–5092
24. Nygaard, T. K., Blouin, G. C., Liu, M., Fukumura, M., Olson, J. S., Fabian, M., Dooley, D. M., and Lei, B. (2006) The mechanism of direct heme transfer from the streptococcal cell surface protein Shp to HtsA of the HtsABC transporter. *J. Biol. Chem.* **281,** 20761–20771
25. Zhu, H., Liu, M., and Lei, B. (2008) The surface protein Shr of *Streptococcus pyogenes* binds heme and transfers it to the streptococcal heme-binding protein Shp. *BMC Microbiol.* **8,** 15
26. Andrade, M. A., Ciccarelli, F. D., Perez-Iratxeta, C., and Bork, P. (2002) NEAT: a domain duplicated in genes near the components of a putative Fe^{3+} siderophore transporter from Gram-positive pathogenic bacteria. *Genome Biol.* **3,** RESEARCH0047
27. Grigg, J. C., Vermeiren, C. L., Heinrichs, D. E., and Murphy, M. E. (2007) Haem recognition by a *Staphylococcus aureus* NEAT domain. *Mol. Microbiol.* **63,** 139–149
28. Villareal, V. A., Pilpa, R. M., Robson, S. A., Fadeev, E. A., and Clubb, R. T. (2008) The IsdC protein from *Staphylococcus aureus* uses a flexible binding pocket to capture heme. *J. Biol. Chem.* **283,** 31591–31600
29. Sharp, K. H., Schneider, S., Cockayne, A., and Paoli, M. (2007) Crystal structure of the heme-IsdC complex, the central conduit of the Isd iron/heme uptake system in *Staphylococcus aureus*. *J. Biol. Chem.* **282,** 10625–10631
30. Villareal, V. A., Spirig, T., Robson, S. A., Liu, M., Lei, B., and Clubb, R. T. (2011) Transient weak protein-protein complexes transfer heme across the cell wall of *Staphylococcus aureus*. *J. Am. Chem. Soc.* **133,** 14176–14179
31. Abe, R., Caaveiro, J. M., Kozuka-Hata, H., Oyama, M., and Tsumoto, K. (2012) Mapping ultra-weak protein-protein interactions between heme transporters of *Staphylococcus aureus*. *J. Biol. Chem.* **287,** 16477–16487
32. Torres, V. J., Pishchany, G., Humayun, M., Schneewind, O., and Skaar, E. P. (2006) *Staphylococcus aureus* IsdB is a hemoglobin receptor required for heme iron utilization. *J. Bacteriol.* **188,** 8421–8429
33. Kim, H. K., DeDent, A., Cheng, A. G., McAdow, M., Bagnoli, F., Missiakas, D. M., and Schneewind, O. (2010) IsdA and IsdB antibodies protect mice against *Staphylococcus aureus* abscess formation and lethal challenge. *Vaccine* **28,** 6382–6392
34. Hargrove, M. S., Whitaker, T., Olson, J. S., Vali, R. J., and Mathews, A. J. (1997) Quaternary structure regulates hemin dissociation from human hemoglobin. *J. Biol. Chem.* **272,** 17385–17389
35. Senturia, R., Faller, M., Yin, S., Loo, J. A., Cascio, D., Sawaya, M. R., Hwang, D., Clubb, R. T., and Guo, F. (2010) Structure of the dimerization domain of DiGeorge critical region 8. *Protein Sci.* **19,** 1354–1365
36. Spirig, T., and Clubb, R. T. (2012) Backbone ^{1}H, ^{13}C, and ^{15}N resonance assignments of the 39 kDa staphylococcal hemoglobin receptor IsdH. *Biomol. NMR Assign.* **6,** 169–172
37. Ascoli, F., Fanelli, M. R., and Antonini, E. (1981) Preparation and properties of apohemoglobin and reconstituted hemoglobins. *Methods Enzymol.* **76,** 72–87
38. Pilpa, R. M., Robson, S. A., Villareal, V. A., Wong, M. L., Phillips, M., and Clubb, R. T. (2009) Functionally distinct NEAT (NEAr Transporter) domains within the *Staphylococcus aureus* IsdH/HarA protein extract heme from methemoglobin. *J. Biol. Chem.* **284,** 1166–1176
39. Cavanagh, J., Fairbrother, W. J., Palmer, A. G., and Skelton, N. J. (1996) *Protein NMR Spectroscopy: Principles and Practice.* Academic Press, San Diego, CA
40. Shen, Y., Delaglio, F., Cornilescu, G., and Bax, A. (2009) TALOS+. A hybrid method for predicting protein backbone torsion angles from NMR chemical shifts. *J. Biomol. NMR* **44,** 213–223
41. Vuister, G. W., and Bax, A. (1993) Quantitative J correlation. A new approach for measuring homonuclear three-bond J(HNH.α.) coupling constants in ^{15}N-enriched proteins. *J. Am. Chem. Soc.* **115,** 7772–7777
42. Delaglio, F., Grzesiek, S., Vuister, G. W., Zhu, G., Pfeifer, J., and Bax, A. (1995) NMRPipe. A multidimensional spectral processing system based on UNIX pipes. *J. Biomol. NMR* **6,** 277–293
43. Garrett, D. S., Powers, R., Gronenborn, A. M., and Clore, G. M. (2011) A common sense approach to peak picking in two-, three-, and four-dimensional spectra using automatic computer analysis of contour diagrams. *J. Magn. Reson.* **213,** 357–363
44. Herrmann, T., Güntert, P., and Wüthrich, K. (2002) Protein NMR structure determination with automated NOE-identification in the NOESY spectra using the new software ATNOS. *J. Biomol. NMR* **24,** 171–189
45. Cornilescu, G., Delaglio, F., and Bax, A. (1999) Protein backbone angle restraints from searching a database for chemical shift and sequence homology. *J. Biomol. NMR* **13,** 289–302
46. Brünger, A. T., Clore, G. M., Gronenborn, A. M., Saffrich, R., and Nilges, M. (1993) Assessing the quality of solution nuclear magnetic resonance structures by complete cross-validation. *Science* **261,** 328–331
47. Laskowski, R. A., Rullmannn, J. A., MacArthur, M. W., Kaptein, R., and Thornton, J. M. (1996) AQUA and PROCHECK-NMR. Programs for checking the quality of protein structures solved by NMR. *J. Biomol. NMR* **8,** 477–486
48. DeLano, W. L. (2006) *The PyMOL Molecular Graphics System*, version 0.99, DeLano Scientific, South San Francisco, CA
49. Goddard, T. D., and Kneller, D. G. (2001) *Sparky NMR Analysis Software*, University of California, San Francisco
50. Krishna Kumar, K., Jacques, D. A., Pishchany, G., Caradoc-Davies, T., Spirig, T., Malmirchegini, G. R., Langley, D. B., Dickson, C. F., Mackay, J. P., Clubb, R. T., Skaar, E. P., Guss, J. M., and Gell, D. A. (2011) Structural basis for hemoglobin capture by *Staphylococcus aureus* cell-surface protein, IsdH. *J. Biol. Chem.* **286,** 38439–38447
51. Pilpa, R. M., Fadeev, E. A., Villareal, V. A., Wong, M. L., Phillips, M., and Clubb, R. T. (2006) Solution structure of the NEAT (NEAr Transporter) domain from IsdH/HarA. The human hemoglobin receptor in *Staphylococcus aureus*. *J. Mol. Biol.* **360,** 435–447
52. Dryla, A., Hoffmann, B., Gelbmann, D., Giefing, C., Hanner, M., Meinke, A., Anderson, A. S., Koppensteiner, W., Konrat, R., von Gabain, A., and Nagy, E. (2007) High-affinity binding of the staphylococcal HarA protein to haptoglobin and hemoglobin involves a domain with an antiparallel eight-stranded β-barrel fold. *J. Bacteriol.* **189,** 254–264
53. Watanabe, M., Tanaka, Y., Suenaga, A., Kuroda, M., Yao, M., Watanabe, N., Arisaka, F., Ohta, T., Tanaka, I., and Tsumoto, K. (2008) Structural basis for multimeric heme complexation through a specific protein-heme

interaction. The case of the third neat domain of IsdH from *Staphylococcus aureus*. *J. Biol. Chem.* **283,** 28649–28659
54. Gaudin, C. F., Grigg, J. C., Arrieta, A. L., and Murphy, M. E. (2011) Unique heme-iron coordination by the hemoglobin receptor IsdB of *Staphylococcus aureus*. *Biochemistry* **50,** 5443–5452
55. Loo, J. A. (2000) Electrospray ionization mass spectrometry. A technology for studying noncovalent macromolecular complexes. *Int. J. Mass Spectrom.* **200,** 175–186
56. Sugita, Y. (1975) Differences in spectra of α and β chains of hemoglobin between isolated state and in tetramer. *J. Biol. Chem.* **250,** 1251–1256
57. Liu, J., and Konermann, L. (2011) Protein-protein binding affinities in solution determined by electrospray mass spectrometry. *J. Am. Soc. Mass Spectrom.* **22,** 408–417
58. Griffith, W. P., and Kaltashov, I. A. (2003) Highly asymmetric interactions between globin chains during hemoglobin assembly revealed by electrospray ionization mass spectrometry. *Biochemistry* **42,** 10024–10033
59. Benesch, R. E., and Kwong, S. (1995) Coupled reactions in hemoglobin. Heme-globin and dimer-dimer association. *J. Biol. Chem.* **270,** 13785–13786
60. Moriwaki, Y., Caaveiro, J. M., Tanaka, Y., Tsutsumi, H., Hamachi, I., and Tsumoto, K. (2011) Molecular basis of recognition of antibacterial porphyrins by heme-transporter IsdH-NEAT3 of *Staphylococcus aureus*. *Biochemistry* **50,** 7311–7320
61. Gouda, H., Torigoe, H., Saito, A., Sato, M., Arata, Y., and Shimada, I. (1992) Three-dimensional solution structure of the B domain of staphylococcal protein A. Comparisons of the solution and crystal structures. *Biochemistry* **31,** 9665–9672
62. Schneider, J. P., Lombardi, A., and DeGrado, W. F. (1998) Analysis and design of three-stranded coiled coils and three-helix bundles. *Fold. Des.* **3,** R29–R40
63. Bunn, F. H., and Forger, B. G. (1986) *Hemoglobin: Molecular, Genetic, and Clinical Aspects*, pg. 21–27, W. B. Saunders Co., Philadelphia
64. Waks, M., Yip, Y. K., and Beychok, S. (1973) Influence of prosthetic groups on protein folding and subunit assembly. Recombination of separated human α- and β-globin chains with heme and alloplex interactions of globin chains with heme-containing subunits. *J. Biol. Chem.* **248,** 6462–6470
65. Lu, C., Xie, G., Liu, M., Zhu, H., and Lei, B. (2012) Direct heme transfer reactions in the group a streptococcus heme acquisition pathway. *PLoS One* **7,** e37556
66. Ouattara, M., Cunha, E. B., Li, X., Huang, Y. S., Dixon, D., and Eichenbaum, Z. (2010) Shr of group A streptococcus is a new type of composite NEAT protein involved in sequestering haem from methaemoglobin. *Mol. Microbiol.* **78,** 739–756
67. Honsa, E. S., Fabian, M., Cardenas, A. M., Olson, J. S., and Maresso, A. W. (2011) The five near-iron transporter (NEAT) domain anthrax hemophore, IsdX2, scavenges heme from hemoglobin and transfers heme to the surface protein IsdC. *J. Biol. Chem.* **286,** 33652–33660
68. Maresso, A. W., Garufi, G., and Schneewind, O. (2008) *Bacillus anthracis* secretes proteins that mediate heme acquisition from hemoglobin. *PLoS Pathog.* **4,** e1000132
69. Thompson, J. D., Gibson, T. J., and Higgins, D. G. (2002) Multiple sequence alignment using ClustalW and ClustalX. *Curr. Protoc. Bioinformatics*, Chapter 2, Unit 2.3
70. Wishart, D. S., Bigam, C. G., Holm, A., Hodges, R. S., and Sykes, B. D. (1995) ^{1}H, ^{13}C, and ^{15}N random coil NMR chemical shifts of the common amino acids. I. Investigations of nearest-neighbor effects. *J. Biomol. NMR* **5,** 67–81

Staphylococcus aureus Uses a Novel Multidomain Receptor to Break Apart Human Hemoglobin and Steal Its Heme

Thomas Spirig, G. Reza Malmirchegini, Jiang Zhang, Scott A. Robson, Megan Sjodt, Mengyao Liu, Kaavya Krishna Kumar, Claire F. Dickson, David A. Gell, Benfang Lei, Joseph A. Loo and Robert T. Clubb

J. Biol. Chem. 2013, 288:1065-1078.
doi: 10.1074/jbc.M112.419119 originally published online November 6, 2012
